

# Ultrafast switching of a spin valve with perpendicular anisotropy

P. Weinberger

*Center for Computational Nanoscience, Seilerstätte 10/22, A1010 Vienna, Austria*

*and Department of Physics, New York University, 4 Washington Place, New York, New York 10003, USA*

(Received 20 January 2010; revised manuscript received 20 February 2010; published 23 March 2010)

The switching properties of a spin valve with perpendicular anisotropy is investigated in terms of the fully relativistic screened Korringa-Kohn-Rostoker method, the corresponding Kubo-Greenwood equation of electric transport, and the Landau-Lifshitz-Gilbert equation. In excellent agreement with very recent experimental data, it is found that (a) the inverse of the switching time is linear with respect to the critical current, (b) the ratio of critical currents for switching from parallel (P) to antiparallel (AP) and from AP to P is about 2, and (c) the tiny magnetoresistance found in experiment is a consequence of the perpendicular anisotropy.

DOI: [10.1103/PhysRevB.81.104417](https://doi.org/10.1103/PhysRevB.81.104417)

PACS number(s): 75.70.-i, 68.37.Ef, 75.47.-m

## I. INTRODUCTION

In the past few years, enormous efforts were made to design devices for fast and high-density nonvolatile magnetic random-access memories, see, e.g., Refs. 1–10. Although the ultimate goal of these efforts seems to be quite clear, namely, to produce thermally stable nanosized magnetic systems preferably to be switched in the picosecond regime reliably by a pulsed current, at present the critical currents to achieve switching appear to be still too large, the switching times too slow and anisotropy effects at room temperature too small. Despite of all attempts made worldwide, a straightforwardly satisfying solution has not emerged. It seems therefore that the search for the most suitable class of systems will go on for quite some time to come.

Up-to-now most theoretical descriptions seem to be based on the original models of Slonczewski<sup>11</sup> and Berger<sup>12</sup> or on the so-called macrospin model and a parametric solution of the Landau-Lifshitz-Gilbert (LLG) equation, see, e.g., Ref. 13. In the following, the switching properties of a spin valve with perpendicular anisotropy, which were studied<sup>10</sup> experimentally only very recently, are investigated on a quantum-mechanical level by means of a fully relativistic *ab initio* approach comprising also the evaluation of switching times as obtained by solving the LLG equation using only *ab initio* parameters. In this study, an attempt is made to model theoretically the experimental system,<sup>10</sup> namely, nanopillars as realistically as possible in terms of a two-dimensional translational invariant system since a real-space description of such systems that would include relativistic effects simply is out of reach.

## II. SYSTEM INVESTIGATED

In Table I, the experimental system is compared with its theoretical realization. In the theoretical description, the Cu leads are represented by semi-infinite Cu(111). Since this system contains two magnetic slabs both orientations of the magnetization (assumed to be uniform in each slab) have to be considered. The corresponding setup is displayed in Table II. Note that in both cases, the orientation of the magnetization varies in the  $xz$  plane,  $\vec{z}$  being the surface normal. This plane is perpendicular to the planes of atoms.

## III. BAND-ENERGY CONTRIBUTION TO THE MAGNETIC ANISOTROPY ENERGY

The band-energy contribution to the magnetic anisotropy energy (free energy at 0 °K) is defined by

$$E_b(\Theta_1, \Theta_2) = E(\Theta_1, \Theta_2) - E(0, 0), \quad (1)$$

where  $\Theta_1, \Theta_2=0$  refers to a reference configuration in which the orientation of the magnetization points uniformly in the whole system along the surface normal (perpendicular to the planes of atoms). It should be noted that  $E_b(\Theta_1, \Theta_2)$  is a function in a two-dimensional function space spanned by the angles  $\Theta_1$  and  $\Theta_2$ . The various paths on the hypersurface of the band energy considered will be denoted in the following as  $[\Theta_1, 0]$ ,  $[0, \Theta_2]$ ,  $[\Theta_1, 90]$ ,  $[90, \Theta_2]$ , and  $[\Theta, \Theta]$ . Furthermore,  $E_b(\Theta_1, \Theta_2)$  refers to the free energy (at 0 °K) per characteristic volume,<sup>14</sup> which in the present case is the volume of the unit cell of an atomic layer in a parent fcc lattice

TABLE I. The experimental and the theoretical system. The conversion to monolayers (MLs) is based on the experimental interlayer spacing in fcc Cu(111), namely, 2.087 Å.

	Experiment (nm)	Experiment (ML)	Theory (ML)
Cu(111)	30	143.75	$\infty$
Cu			12
Pt	3	14.37	14
$4 \times \begin{bmatrix} \text{Co} \\ \text{Pt} \end{bmatrix}$	0.25	1.20	1
	0.52	2.49	2
Co	0.25	1.20	1
$2 \times \begin{bmatrix} \text{Ni} \\ \text{Co} \end{bmatrix}$	0.6	2.87	2
	0.1	0.47	1
Cu	4	19.16	19
$2 \times \begin{bmatrix} \text{Co} \\ \text{Ni} \end{bmatrix}$	0.1	0.47	1
	0.6	2.87	2
Co	0.25	1.20	1
Pt	3	14.37	14
Cu			11
Cu(111)	20	95.83	$\infty$

TABLE II. Orientation of the magnetization.  $\Theta_1$  and  $\Theta_2$  are rotations angles around the in-plane  $y$  axis,  $0 \leq \Theta_1, \Theta_2 \leq 180$ .

Part of system	Rotation angle
Cu(111)/Cu <sub>12</sub> /Pt <sub>11</sub>	0
Pt <sub>3</sub> /(CoPt <sub>2</sub> ) <sub>4</sub> /Co/(Ni <sub>2</sub> Co) <sub>2</sub> /Cu <sub>3</sub>	$\Theta_1$
Cu <sub>13</sub>	0
Cu <sub>3</sub> (CoNi <sub>2</sub> ) <sub>2</sub> /Co/Pt <sub>n</sub> /Cu <sub>3</sub>	$\Theta_2$
Cu <sub>8</sub> /Cu(111)	0

of Cu spacing ( $a^3/4$ ) times the number of atomic layers considered (81). It is important to note that  $E_b(\Theta_1, \Theta_2)$  has to be an intrinsic quantity, which in turn means that by adding an arbitrary number of atomic layers  $E_b(\Theta_1, \Theta_2)$  has to remain constant. Adding therefore, e.g., additional Cu lead layers has no effect at all.

From Fig. 1 in which the band energy along these paths is displayed, one easily can see that  $E_b(90, 0) < E_b(0, 90)$  but also that  $E_b(\Theta_1, 90) \geq E_b(0, 90)$ ,  $\Theta_1 \leq 90^\circ$ . In all cases, a positive maximum is present, indicating that stable switching between the state at  $\Theta_1, \Theta_2 = 0$  and that at 180 can be achieved. It should be noted, in particular, that for  $\Theta < 60$  and  $\Theta > 120$ , there is virtually no energy difference between the paths  $[\Theta, 0]$  and  $[0, \Theta]$ , i.e., one cannot state which of the magnetic slabs “moves.” Both rotated simultaneously, however, correspond to a much higher band energy. Quite clearly the band energy along a particular path  $[\Theta_1, \Theta_2]$ , say  $[\Theta_1, 0]$ , can be expanded as

$$E_b(\Theta_1, 0) = \sum_{s=0}^k a_s [\Theta_1, 0] \cos^s(\Theta_1), \quad (2)$$

where the coefficients  $a_s[\Theta_1, 0]$  can easily be found from an appropriate polynomial fit.

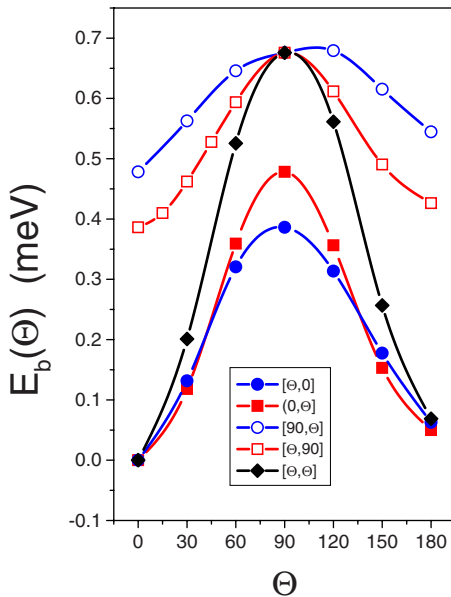


FIG. 1. (Color online) Band-energy contribution to the anisotropy energy. The angles  $\Theta_1$  and  $\Theta_2$  are marked explicitly.

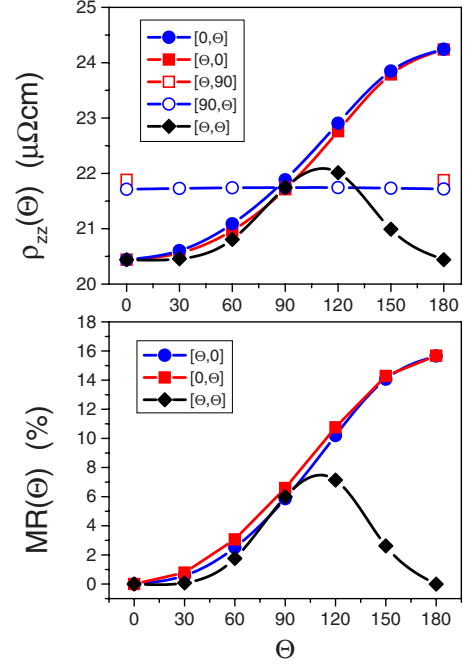


FIG. 2. (Color online) Resistivity (top) and magnetoresistance (bottom) along indicated paths.

#### IV. MAGNETORESISTANCE

The magnetoresistance (MR) is defined in here as

$$\text{MR}(\Theta_1, \Theta_2) = \frac{r(\Theta_1, \Theta_2) - r(0, 0)}{r(\Theta_1, \Theta_2)}, \quad (3)$$

$$r(\Theta_1, \Theta_2) = L \rho_{zz}(\Theta_1, \Theta_2), \quad (4)$$

where  $r(\Theta_1, \Theta_2)$  is the so-called sheet resistance,  $\rho_{zz}(\Theta_1, \Theta_2)$  the  $zz$ -like element of the resistivity tensor, and  $L$  the total number of atomic planes in the spin valve considered (96 in the present context). Clearly, also the  $\text{MR}(\Theta_1, \Theta_2)$ ,  $r(\Theta_1, \Theta_2)$  and  $\rho_{zz}(\Theta_1, \Theta_2)$  form surfaces in the function space spanned by  $\Theta_1$  and  $\Theta_2$ . In Fig. 2,  $\rho_{zz}(\Theta_1, \Theta_2)$  and the corresponding magnetoresistance are displayed. Note that of course as for all other quantities the temperature is  $0^\circ \text{K}$ .

The fact that along paths  $[\Theta_1, 90]$  and  $[90, \Theta_2]$ , the resistivity is nearly unchanged results mainly from the properties of the layer-off-diagonal elements  $\sigma_{zz}^{ij}(\Theta_1, \Theta_2)$  of the conductivity tensor,

$$\sigma_{zz}(\Theta_1, \Theta_2) = \sum_{i,j} \sigma_{zz}^{ij}(\Theta_1, \Theta_2)$$

which fall off rapidly as  $|i-j|$  increases.<sup>14,15</sup> Since the thickness of the Cu spacer is rather very large in the present system, an interaction between the two magnetic slabs is hardly to be seen in  $\sigma_{zz}(\Theta_1, \Theta_2)$  or  $\rho_{zz}(\Theta_1, \Theta_2)$ . On the other hand, going separately along either  $[\Theta_1, 0]$  or  $[0, \Theta_2]$ , the usual  $(1 - \cos \Theta)$  kind behavior seems to apply, provided of course that they would refer to the minimal free-energy path. Since according to Fig. 1, the stable states are when the orientation of the magnetization is either uniformly parallel

TABLE III. Averaged spin moments ( $\mu_B$ ). The column to the left indicates the atomic layers and their weights over whose magnetic moment was averaged. For details see text.

Averaging over	$M$ ( $\mu_B$ )
Pt <sub>3</sub> /(CoPt <sub>2</sub> ) <sub>4</sub> /(CoNi <sub>2</sub> ) <sub>2</sub> /Co/Cu <sub>3</sub>	0.70306
Pt <sub>1</sub> /(CoPt <sub>2</sub> ) <sub>4</sub> /(CoNi <sub>2</sub> ) <sub>2</sub> /Co/Cu <sub>0</sub>	0.83784
Pt <sub>0</sub> /(CoPt <sub>2</sub> ) <sub>4</sub> /(CoNi <sub>2</sub> ) <sub>2</sub> /Co/Cu <sub>0</sub>	0.91428
Pt <sub>0</sub> /(CoPt <sub>2</sub> ) <sub>0</sub> /(CoNi <sub>2</sub> ) <sub>0</sub> /Co/Cu <sub>0</sub>	1.68545
Cu <sub>3</sub> /(CoNi <sub>2</sub> ) <sub>2</sub> /Co/Pt <sub>3</sub>	0.63603
Cu <sub>0</sub> /(CoNi <sub>2</sub> ) <sub>2</sub> /Co/Pt <sub>1</sub>	1.03074
Cu <sub>0</sub> /(CoNi <sub>2</sub> ) <sub>2</sub> /Co/Pt <sub>0</sub>	1.15331
Cu <sub>0</sub> /(CoNi <sub>2</sub> ) <sub>0</sub> /Co/Pt <sub>0</sub>	1.68061

or uniformly antiparallel to the surface normal, i.e., when  $\Theta_1, \Theta_2=0$  or  $\Theta_1, \Theta_2=180$ , path  $[\Theta, \Theta]$  finally shows that the corresponding MR is minute.

## V. COMPUTATIONAL DETAILS

All *ab initio* calculations were performed using the spin-polarized relativistic screened Korrington-Kohn-Rostoker method.<sup>16</sup> The effective potentials and exchange fields were calculated self-consistently at the experimental lattice spacing of fcc Cu using 45  $k$  points in irreducible part of the surface Brillouin zone (ISBZ) by placing the orientation of the magnetization uniformly along  $\vec{z}$  (surface normal). In using these potentials and exchange fields, the free energy in Eq. (1) was evaluated<sup>16</sup> by means of a contourintegration along a semicircle using a 16-point Gaussian quadrature and 1830  $k$  points per ISBZ. The electric-transport properties were evaluated at complex Fermi energies by means of the fully relativistic Kubo equation<sup>14,16</sup> using also 1830  $k$  points per ISBZ, and then analytically continued to the real axis.

## VI. LLG EQUATION

Whenever one uses the LLG equation,

$$\frac{d\vec{M}}{dt} = -\gamma\vec{M} \times \vec{H}_{eff} + \alpha\vec{n} \times (\vec{M} \times \vec{H}_{eff}), \quad (5)$$

$$\vec{n} = \frac{\vec{M}}{M}, \quad M = |\vec{M}|, \quad \vec{n} \in xz \text{ plane}, \quad (6)$$

where  $\gamma$  is the gyromagnetic ratio and  $\alpha = \alpha_G \gamma / (1 + \alpha_G^2)$ ,  $\alpha_G$  being the Gilbert damping factor, one ought to remember that in this equation,  $\vec{M}$  is a macroscopic quantity resulting from an average over microscopic quantities. In changing  $\vec{M}$  in one of the magnetic slabs, an average over the magnetic moments  $\vec{m}_i$  of those  $N$  atomic layers forming a particular magnetic slab has to be performed, see also Table III,

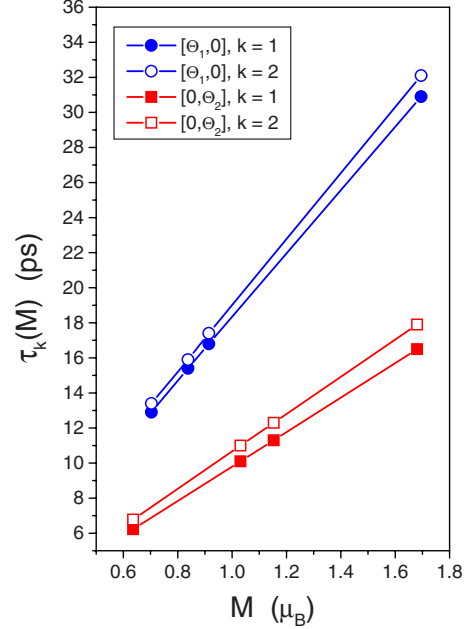


FIG. 3. (Color online) Dependence of the switching time along  $[\Theta_1, 0]$  and  $[0, \Theta_2]$  on the averaged moment  $M$ .

$$\vec{M} = \frac{1}{N} \sum_{i=1}^N \vec{m}_i. \quad (7)$$

In Eq. (5), the internal field  $\vec{H}_{eff}$  is given<sup>17</sup> by the derivative of the band energy with respect to  $\vec{M}$ ,

$$\vec{H}_{eff} = -\frac{1}{M} \frac{\partial E_b}{\partial \vec{M}}. \quad (8)$$

As is well known for the switching time, i.e., for the time needed to move from an initial orientation  $\vec{n}_i$  to a final one  $\vec{n}_f$ ,<sup>17</sup> it is sufficient to consider only the second term in the LLG equation, namely,

$$\frac{d\vec{M}}{dt} \simeq \alpha\vec{n} \times (\vec{M} \times \vec{H}_{eff}). \quad (9)$$

In using an integration interval  $[n_i, n_f] = [\cos \Theta_i, \cos \Theta_f]$ , one then obtains the corresponding switching time. For matters of simplicity, in the following, switching times corresponding to the integration intervals  $[1, 0]$  and  $[-1, 0]$  are denoted by  $\tau_1(M)$  and  $\tau_2(M)$ , respectively. Since in Eq. (9),  $\alpha$  is an empirical parameter,<sup>18</sup> for which up-to-now no quantum-mechanical expression was found, and, since most likely a reliable experimental value for the system under investigation is presently not available, in here  $\alpha$  was chosen to be unity.

In Fig. 3, it is shown that  $\tau_1(M)$  as well as  $\tau_2(M)$  vary linearly with the corresponding averaged magnetic moment  $M$ , see Eq. (7) and Table III. It should be noted that the total switching time between  $\Theta_i=0^\circ$  and  $\Theta_f=180^\circ$ , i.e., in the interval  $[1, -1]$  is of course defined by

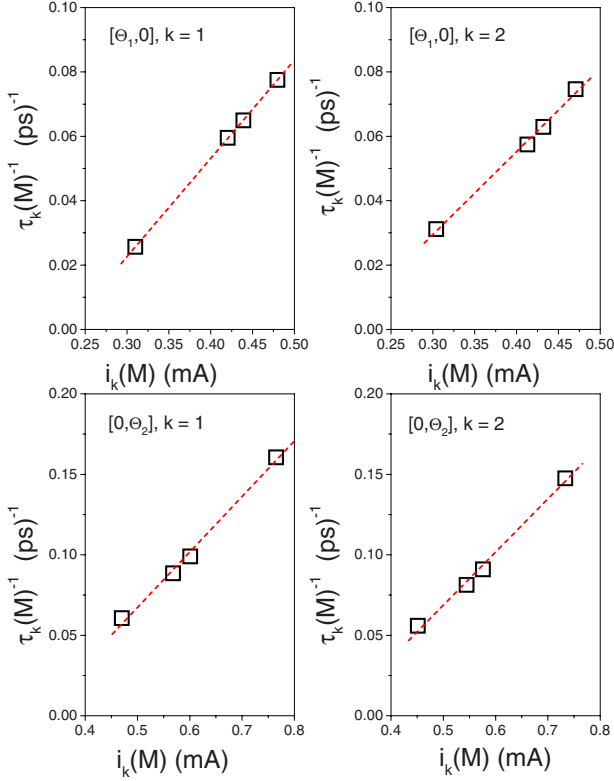


FIG. 4. (Color online) Switching time as a function of the current along different paths. The dashed lines refer to a linear fit of the form  $\tau_k^{-1}(M) = a + bi_k(M)$ . Switching from parallel to perpendicular to the surface normal is denoted by  $k=1$ , switching from antiparallel to perpendicular by  $k=2$ .

$$\tau(M) = \tau_1(M) + \tau_2(M). \quad (10)$$

## VII. CURRENT

The current needed to switch the orientation of the magnetization along a particular path on the band-energy hypersurface and reflecting a particular integration interval  $k$  can be obtained approximately from the maximum band energy along this path and the corresponding sheet resistance.<sup>17</sup> Consider, for example, paths  $[\Theta_1, 0]$  and  $[0, \Theta_2]$  then the critical currents are given by

$$i_k(M) = \sqrt{\frac{A_0}{\tau_k(M)}} \left\{ \frac{[E_b(90,0)/r(90,0)]^{1/2}}{[E_b(0,90)/r(0,90)]^{1/2}} \right\},$$

where  $A_0$  is the unit area and  $\tau_k(M)$  is the time needed to reach the respective maximum in  $E_b(\Theta_1, \Theta_2)$  either from a configuration uniformly parallel ( $k=1$ ) or uniformly antiparallel ( $k=2$ ) to the surface normal. Assuming in accordance with Ref. 10, a unit area of  $A_0 = 100 \times 100$  (nm)<sup>2</sup> for matters of comparison to the experiment the inverse of the switching time  $\tau_k(M)$  is shown in Fig. 4 as a function of corresponding critical current  $i_k(M)$ . It is interesting to note that the evaluated data points fit quite well a linear form of the type  $\tau_k^{-1}(M) = a + bi_k(M)$ .

In order to understand the complicated switching in this spin valve, one has to go back to Fig. 1 and view the various

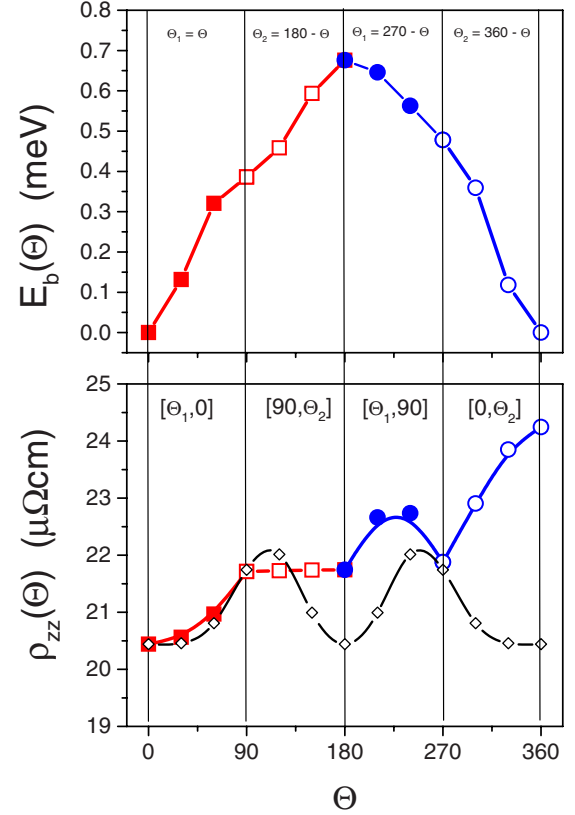


FIG. 5. (Color online) Unfolding the band energy (top) and the resistivity (bottom). In each part of these figures, the orientation of the magnetization changes along a particular path. For comparison in the lower part of the figure also  $\rho_{zz}(\Theta, \Theta)$  (open diamonds) is shown.

paths separately as shown in the upper part of Fig. 5. Starting from  $\Theta_1, \Theta_2 = 0$ , namely, considering first the case  $k=1$ , by increasing the current, the system starts to move along  $[\Theta_1, 0]$  and then along  $[90, \Theta_2]$  until a uniform in-plane orientation  $[90, 90]$  is reached, from which it can drop down to  $\Theta_1, \Theta_2 = 180$  on the fastest path, e.g., first along  $[0, \Theta_2]$  and then along  $[\Theta_1, 90]$  or collectively along  $[\Theta, \Theta]$ . Switching back, i.e., starting at  $\Theta_1, \Theta_2 = 180$  case  $k=2$  applies. In the lower part of Fig. 5, the corresponding resistivities are shown together with  $\rho_{zz}(\Theta, \Theta)$ . Along each path, the corresponding switching time and critical current are listed in Table IV; the magnetoresistance at the end points of these paths are collected in Table V.

The surprisingly long-time spend on path  $[90, \Theta_2]$  can easily be explained by inspecting the expansion coefficients for the band energy in Eq. (2). From Fig. 6, it becomes evident that path  $[90, \Theta_2]$  is the only one with nearly no anisotropy contribution, which of course is the very reason for the slow movement.

Finally, by putting all information available together in Fig. 7, the necessary currents to force the system from parallel (P) to antiparallel (AP), and back are shown. Switching from P to AP ( $k=1$ ) by rotating the first magnetic slab and then approach a uniform in-plane orientation requires 0.478 mA whereas via a rotation of the second magnetic slab 0.68 mA are needed, see also Table IV. Switching from AP to P

TABLE IV. Switching times and currents corresponding to the integration intervals  $[1,0]$ ,  $[0,-1]$ , and  $[1,-1]$ . In the case of the first slab, an averaged magnetic moment of  $0.91428\mu_B$  applies, in the case of the second one  $1.15331\mu_B$ , along path  $[\Theta, \Theta]$  the arithmetic mean.

	Magnetic slab	Integration intervall	$k$	$\tau_k(M)$ (ps)	$i_k(M)$ (mA)
P → AP	1	$[1,0]$	1	15.2	0.441
		$[0,-1]$	2	97.0	0.037
		$[1,-1]$		112.2	0.478
	2	$[1,0]$	1	11.3	0.569
		$[0,-1]$	2	24.4	0.114
		$[1,-1]$		35.7	0.683
AP → P	1	$[-1,0]$	1	18.8	0.246
		$[0,1]$	2	293.0	0.014
		$[-1,1]$		311.8	0.260
	2	$[1,0]$	1	12.3	0.377
		$[0,-1]$	2	10.7	0.145
		$[1,-1]$		23.0	0.522
P → AP and AP → P	1 and 2	$[1,0]$	1	8.8	0.77
		$[0,-1]$	2	9.6	0.73

( $k=2$ ) needs 0.25 mA and 0.52 mA, respectively. Note that when switching from AP to P, the current to be applied starts of course again at zero. The ratios of critical currents (P/AP) is then given by 1.91 rotating the first magnetic slab and 1.31 for the second one.

VIII. COMPARISON TO THE EXPERIMENTAL DATA

When comparing the theoretical results with the experimental data in Ref. 10, one has to keep in mind that (1) the experimental samples were prepared by combining e-beam and optical lithography and (2) the measurements were carried out at room temperature. The samples are therefore of little known interlayer spacing and most likely exhibit lots of structural defects. At room temperature, anisotropy effects are usually substantially smaller than at very low temperatures, the measured currents in turn reflect to quite some extend contributions due to phonons. There are very few theoretical studies on the temperature dependence of the anisotropy energy in layered structures, see, e.g., Ref. 19, indicating that at room temperature, the anisotropy energy is most likely between about 30–50 % less than the value at 0 °K. Studies of the temperature dependence of conductivities in magnetic materials are even rarer,<sup>20</sup> for layered structures there is presently none. Very little is known also about

relaxation effects for electric-transport properties in spin valves. Preliminary studies<sup>21</sup> of changing the interlayer distance in the present system proved that the ratio of currents discussed in the context of Fig. 7 seems not to be changing.

The calculated positive maximum in the band energy is in turn 0.386, 0.478, and 0.676 meV for  $[90,0]$ ,  $[0,90]$ , and  $[90,90]$ . Because of these maxima, both the parallel (P;  $\Theta_1, \Theta_2=0$ ) as well as the antiparallel state (AP;  $\Theta_1, \Theta_2=180$ ) are stable magnetic configurations and guarantee reliable switching. It should be noted that, in principle, the magnetic anisotropy energy contains of course also a magnetic dipole-dipole contribution (shape anisotropy), which, however, is not reflected in the electric properties. The band energy can therefore be regarded as the leading effect of the

TABLE V. Magnetoresistance  $MR(\Theta_1; \Theta_2)$  (%) at the end points of the paths considered.

Path	$\Theta=90^\circ$	$\Theta=180^\circ$
$[\Theta, 0]$	5.8	15.7
$[0, \Theta]$	6.6	15.7
$[\Theta, \Theta]$	6.0	~0

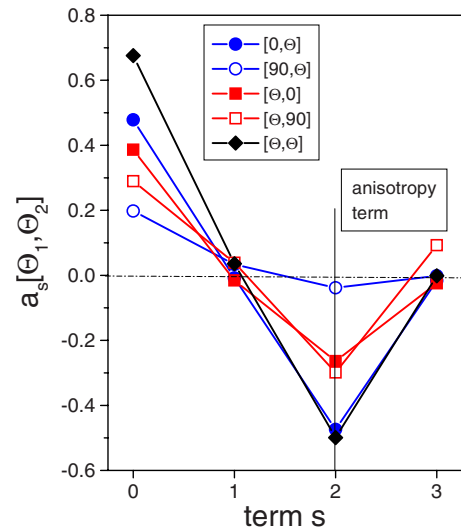


FIG. 6. (Color online) Expansion coefficients for the power series in  $\cos \Theta$  of the band energy, see Eq. (2).

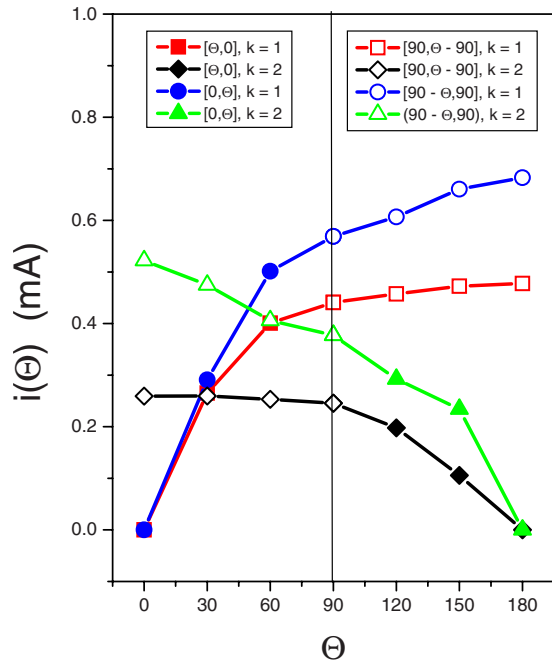


FIG. 7. (Color online) Currents along various paths (indicated). Ascending (squares and circles) from left to right corresponds to a switching from P to AP and descending (diamonds and triangles) from AP to P. All four curves start at  $\Theta=0^\circ$  and end at  $\Theta=180^\circ$  (or vice versa).

perpendicular magnetic anisotropy as far as the electric properties are concerned.

Experimentally it is found<sup>10</sup> that “the critical current to switch from P to AP is 6.8 mA and from AP to P 3.2 mA, and the MR is 0.3%.” The ratio of the experimental critical currents,  $i_P/i_{AP}$ , is 2.12, which compares surprisingly well with

the above-quoted value of 1.91 (first magnetic slab). Obviously, the MR found experimentally is rather very small, which, however, is quite understandable since the possible theoretical values of the theoretical MR values are very close to zero, see also Table V. Definitely in the experiment, neither the switching of only one of the magnetic slabs is observed because otherwise the MR would be quite a bit higher, see Fig. 2 and Table V. Furthermore, the inverse of the switching times  $\tau_k(M)$  is linear in  $i_k(M)$ , see Fig. 4, and is therefore exactly of the same form as shown in Fig. 2b of Ref. 10 and as proposed in Eq. (2) of these authors.

It seems therefore most probable that the switching properties in this spin valve are caused mainly by the first magnetic slab rather than by the second one, which in turn is rather surprising and might contradict intuitive thinking. Although the very low MR, the functional form of  $\tau_k^{-1}(M)$  with respect to  $i_k(M)$ , the  $i_P/i_{AP}$  ratio, and *grosso modo* even the magnitude of the critical current appear to be in rather very good agreement with the experimental results of Ref. 10, one has to remember that finite-temperature effects and structural defects were not accounted for in the theoretical description. In summary, however, it can be said that the applied quantum-mechanical approach and the multiscaling in terms of the LLG equation yield a very detailed, coherent interpretation of experimentally found switching properties in a rather sophisticated spin valve with perpendicular anisotropy.

#### ACKNOWLEDGMENTS

I would like to thank A. Kent (NYU) for the discussions we had concerning the experimental data and the Department of Physics of the New York University for the hospitality I enjoyed in the last years.

- <sup>1</sup>S. Mangin, Y. Henry, D. Ravelosona, J. A. Katine, and E. E. Fullerton, *Nature Mater.* **5**, 210 (2006).
- <sup>2</sup>J. A. Katine and E. E. Fullerton, *J. Magn. Magn. Mater.* **320**, 1217 (2008).
- <sup>3</sup>O. Ozatay, P. G. Gowtham, K. W. Tan, J. C. Read, K. A. Mkhoyan, M. G. Thomas, and G. D. Fuchs, *Nature Mater.* **7**, 567 (2008).
- <sup>4</sup>S. Garzon, L. Ye, R. A. Webb, T. M. Crawford, M. Covington, and S. Kaka, *Phys. Rev. B* **78**, 180401(R) (2008).
- <sup>5</sup>T. Devolder, J. Hayakawa, K. Ito, H. Takahashi, S. Ikeda, P. Crozat, N. Zerounian, J.-V. Kim, C. Chappert, and H. Ohno, *Phys. Rev. Lett.* **100**, 057206 (2008).
- <sup>6</sup>O. J. Lee, V. S. Pribiag, P. M. Braganca, P. G. Gowtham, D. C. Ralph, and R. A. Buhrman, *Appl. Phys. Lett.* **95**, 012506 (2009).
- <sup>7</sup>C. Papusoi, B. Delaët, B. Rodmacq, D. Houssameddine, J.-P. Michel, and U. Ebels, *Appl. Phys. Lett.* **95**, 072506 (2009).
- <sup>8</sup>S. Mangin, Y. Henry, D. Ravelosona, J. A. Katine, E. E. Fullerton, R. C. Sousa, L. Buda-Prejbeanu, and B. Dieny, *Appl. Phys. Lett.* **94**, 012502 (2009).
- <sup>9</sup>P. P. Horley, V. R. Vieira, P. Gorley, J. González Hernández, V. K. Dugaev, and J. Barnaś, *J. Phys. D* **42**, 245007 (2009).
- <sup>10</sup>D. Bedau, H. Liu, J.-J. Bouzagliou, A. D. Kent, J. Z. Sun, J. A. Katine, E. E. Fullerton, and S. Mangin, *Appl. Phys. Lett.* **96**,

022514 (2010).

- <sup>11</sup>J. C. Slonczewski, *J. Magn. Magn. Mater.* **159**, L1 (1996).
- <sup>12</sup>L. Berger, *Phys. Rev. B* **54**, 9353 (1996).
- <sup>13</sup>P. Baláz, M. Gmitra, and J. Barnaś, *Phys. Rev. B* **79**, 144301 (2009).
- <sup>14</sup>P. Weinberger, *Magnetic Anisotropies in Nanstructured Matter* (CRC, Boca Raton, London, New York, 2008).
- <sup>15</sup>C. Blaas, L. Szunyogh, P. Weinberger, C. Sommers, P. M. Levy, and J. Shi, *Phys. Rev. B* **65**, 134427 (2002).
- <sup>16</sup>J. Zabloudil, R. Hammerling, L. Szunyogh, and P. Weinberger, *Electron Scattering in Solid Matter* (Springer, Berlin, New York, 2004).
- <sup>17</sup>P. Weinberger, A. Vernes, B. L. Gyorffy, and L. Szunyogh, *Phys. Rev. B* **70**, 094401 (2004); A. Vernes, P. Weinberger, and L. Szunyogh, *ibid.* **72**, 012401 (2005).
- <sup>18</sup>The effect of using different empirical values of  $\alpha$  in Eq. (9) for one and the same system is discussed in Ref. 17(a).
- <sup>19</sup>A. Buruzs, L. Szunyogh, P. Weinberger, and J. B. Staunton, *J. Magn. Magn. Mater.* **316**, e371 (2007); Á. Buruzs, P. Weinberger, L. Szunyogh, L. Udvardi, P. I. Chleboun, A. M. Fischer, and J. B. Staunton, *Phys. Rev. B* **76**, 064417 (2007).
- <sup>20</sup>A. Buruzs, L. Szunyogh, and P. Weinberger, *Philos. Mag.* **88**, 2615 (2008).
- <sup>21</sup>P. Weinberger (unpublished).